

Calculations of the susceptibility of interacting superparamagnetic particles

R. W. Chantrell and N. Walmsley

Physics Department, Durham University, South Road, Durham, DH1 3LE, United Kingdom

J. Gore and M. Maylin

Structural Materials Centre, DERA, Ively Road, Farnborough, Hants, GU14 0LX, United Kingdom

(Received 6 March 2000; published 15 December 2000)

A model of the magnetic properties of a dispersion of interacting superparamagnetic particles in a solid matrix is presented. The model uses Monte Carlo techniques and is capable of predicting the time and temperature dependence of the magnetic properties. The model is applied to the study of the magnetic behavior of a cobalt granular system, particularly the low-field susceptibility. It is shown that strongly interacting systems at high density exhibit non-Langevin behavior and give a strongly nonlinear variation of susceptibility with packing density. The temperature dependence of the initial susceptibility shows the characteristic peak observed experimentally, with the peak temperature increasing with packing density. The field cooled (FC) and zero field cooled (ZFC) magnetization are also studied. The field dependence of the FC magnetization is shown to depend on the interparticle interactions and also on the orientational easy axis distribution. The FC magnetization is found to exhibit a peak resulting from the interactions. This behavior is finally related to the energy barrier distribution of the system (and its dependence on the interactions) using the temperature decay of remanence. It is also shown that the remanence calculated from the complete hysteresis loop at each temperature differs from the values obtained by increasing the temperature of a system initially at saturation remanence. The evolution of magnetic properties as a function of the magnetic state and history points to the importance of collective phenomena. Calculations of a spin-spin correlation function show the existence of a state with short-ranged order at low temperatures.

DOI: 10.1103/PhysRevB.63.024410

PACS number(s): 75.50.Lk, 75.50.Mm

I. INTRODUCTION

The magnetic properties of a fine particle system are strongly dependent on the interactions between the particles. Clearly the magnetostatic interaction between particles might be expected to be significant, especially at high densities. In addition, in materials consisting of magnetic particles in a conducting (nonmagnetic) medium, the possibility exists of a reduced exchange coupling between the grains. The effects of interactions are, in general, complex. A number of previous analytical treatments have been carried out.¹⁻⁷ In particular, the effects of interactions on the dynamic (relaxational) behavior have been studied, and the results applied, for example, to the understanding of the variation of the initial susceptibility with temperature. However, it is clear that these approaches involve significant approximations, whose actual effects are not easy to determine. There exists considerable discussion in the literature as to the correct approach. Within this context there would appear to be a need for computational studies to provide results on “model” systems for comparison with analytical theory, and with experimental data. Chantrell *et al.*⁸ developed a Monte Carlo model and studied the hysteresis properties of systems produced by the solidification of ferrofluids. In this case a standard Metropolis type MC model was used to predict the microstructure of the ferrofluid which was assumed to be frozen in when the ferrofluid was solidified. These calculations showed that in strongly interacting systems some phase separation is possible which leads to the presence of aggregates even in systems of low packing density. The remanent state was shown to be strongly dependent on the magneto-

static interactions between particles. Andersson *et al.*⁹ have used a similar Monte Carlo model to investigate theoretically the behavior of a collection of interacting particles. The system was assumed to be monodispersed, but some disorder was introduced via a random orientation of easy axes and via a random placement of particles in the computational cell. Calculations of the dynamic susceptibility were made, leading to the prediction of a collective magnetic state, which is reflected in the appearance of magnetic aging, manifested by a dependence of the slow dynamic behavior on the “waiting time” after quenching to a low temperature before the probe field is applied. This effect has also been observed experimentally.¹⁰ MC calculations were also carried out by Kechrakos and Trohidou¹¹ of the hysteresis behavior of interacting fine particle systems. This work shows a complex behavior, dependent on the detailed balance between the anisotropy and interaction energies, for example a purely dipolar system (zero anisotropy) was shown to exhibit an increase in coercivity at low packing density, leading to a peak at the percolation threshold.

The effects of interactions on the magnetic behavior of fine particle systems were reviewed by Chantrell *et al.*¹² Essentially, the behavior of such a system is dominated by a critical diameter which determines the transition from reversible superparamagnetic (SPM) to irreversible or thermally stable (TS) behavior. For a system of particles with uniaxial anisotropy and easy axes aligned with the field there exists an energy barrier to magnetization reversal given by $E_b = KV(1 - H/H_k)^2$, where H is the applied field, K is the anisotropy energy density, and V is the particle volume. $H_k = 2K/I_{sb}$ (with I_{sb} the saturation magnetization of the bulk

material of which the particles are composed) is the anisotropy field. H_k is essentially the intrinsic coercivity of the particles, i.e., the coercivity in the absence of thermal activation. At a nonzero temperature, there exists the probability of a thermally activated transition over the energy barrier. This process gives rise to a characteristic relaxation time given by the Arrhenius-Neel Law¹³

$$\tau^{-1} = f_0 \exp(-E_b/kT), \quad (1)$$

where f_0 is a frequency factor, of the order of the precession frequency of the magnetic moment, often taken as 10^9 s^{-1} . In zero field, setting the relaxation time equal to some characteristic measurement time t leads to the expression $V_c = Ln(tf_0)kT/K$ with V_c a critical volume for SPM behavior. The rapid variation of τ with E_b is responsible for a separation of the magnetic behavior into two distinct ‘‘phases;’’ the SPM phase for $V < V_c$ which, having $t \gg \tau$ is able to achieve thermal equilibrium, and conversely the thermally stable (TS) phase which exhibits irreversible magnetic behavior. The measurement most clearly illustrating the change from TS to SPM behavior is the temperature dependence of the low-field susceptibility. Here, the gradual change from TS to SPM behavior with increasing temperature results in a characteristic susceptibility peak occurring at a temperature which increases with the packing density of the particles.

Clearly the relative balance of the two phases is responsible for determining the magnetic behavior of the system and the properties of each phase must be simulated within a physically meaningful model. It is also important to note that the two phases cannot be considered in isolation, since in general their behavior is linked by the interparticle interactions. The theoretical description of both SPM and TS phases requires very different approaches. Here, we develop a Monte Carlo model, based upon the calculation of transition probabilities, which is able to predict the behavior of a general fine particle system consisting of any arbitrary value of the SPM and TS fractions. As a consequence the temperature and time dependence of the magnetic properties are naturally included.

It is the aim of the current paper to present the results of a computational study based on a model of an interacting fine particle system using Monte Carlo techniques. The model is applied first to a study of the initial susceptibility and its dependence on packing density. Further calculations of the variation of susceptibility with temperature are also carried out, in order to provide a more detailed picture of the interaction effects. This aspect of the investigation is also of importance since there exists a substantial body of experimental evidence to suggest that interactions have a strong bearing on this property. Finally, we relate these results to the underlying energy barrier distribution of the system, and especially its dependence on interparticle interactions.

II. THE MONTE CARLO MODEL

Fundamentally, magnetization reversal proceeds via thermal activation over the anisotropy energy barrier. However, the energy barrier is dependent upon the interparticle interactions. In this model thermal effects are introduced via the

Arrhenius-Neel relaxation time, with an energy barrier dependent on the local field, by means of which interaction effects are introduced. Given that interactions are introduced by means of a local field, the model cannot correctly take into account strong collective modes of magnetization reversal which may occur in highly ordered systems, and is thus most applicable to materials with some local disorder, into which category many fine particle systems fall. In this study we consider systems with disordered microstructures. The model consists of a cubic cell in which the positions of the particles are generated randomly with the constraint that particle overlap is not allowed. This was achieved by assigning (x, y, z) coordinates uniformly in the range $0 < \alpha < L$ with α the coordinate and L the size of the cubic computational cell. Assignments leading to overlap with an existing particle were rejected and a further trial made. A particle size distribution was introduced, with the particle sizes being selected according to a lognormal distribution function. In order to achieve high packing densities the particles were assigned to the cell in decreasing order of particle diameter, allowing smaller particles to occupy the interstitial sites between the larger particles. The anisotropy easy axes were generated randomly in 3D, i.e., with a probability for the polar angle $p(\theta_a) = \sin(\theta_a)$ and a uniformly random distribution of the equatorial axis ϕ_a . Periodic boundary conditions were applied in 3D in order to remove boundary effects. The total energy of a particle can be written as

$$E = KV(\mathbf{e} \cdot \mathbf{m})^2 - \boldsymbol{\mu} \times \mathbf{H}_T, \quad (2)$$

where the unit vectors \mathbf{e} and \mathbf{m} represent the orientation of the local anisotropy easy axis and the magnetization respectively, and the calculations are done in polar coordinates, specifically $\boldsymbol{\mu} = \mu(\theta, \phi)$. The total local field \mathbf{H}_T acting on each particle is the sum of the applied field and the dipolar field arising from the neighboring particles, given by

$$\mathbf{H}_T = H_a \hat{z} + \sum_{i \neq j} \left[\frac{3(\boldsymbol{\mu}_j \cdot \mathbf{r}_{ij})\mathbf{r}_{ij}}{d_{ij}^5} - \frac{\boldsymbol{\mu}_j}{d_{ij}^3} \right], \quad (3)$$

where the applied field is chosen to be along the z axis. The second term of Eq. (3) represents the vector sum of the total dipolar fields arising from neighboring particles. $\mathbf{r}_{ij} = d_{ij} \hat{r}_{ij}$ is the position vector of the particles i relative to j where \hat{r}_{ij} is a unit vector in the direction of the particle separation d_{ij} . The dipolar field is calculated within a spherical volume defined by a cutoff radius chosen to be at a distance six times the mean radius of the particles. In the systems considered here, extension of the cutoff range had no significant effect on the predictions of the calculations, consistent with the results of Andersson *et al.*⁹ Long-range magnetostatic interactions were introduced using an effective field term.

The behavior of small SPM particles (for which the energy barrier was $\leq 3kT$) was simulated using a standard Metropolis algorithm.¹⁴ The total energy of a particle within the cell (anisotropy and Zeeman) is given from Eq. (2) by

$$E = KV \sin^2 \alpha - \mu H_T \cos \beta, \quad (4)$$

where the first term represents the anisotropy energy (uniaxial) and the second term the total Zeeman energy (includ-

ing the applied and interaction fields), with μ the magnetic moment. The angles α and β represent the angles between the moment and the easy axis and the total field acting on the particle, respectively.

The Metropolis algorithm proceeds by changing the moment orientation of each particle by a random amount and allowing the change with a probability $\min[1, \exp(-\Delta E/kT)]$. For each particle θ and ϕ are incremented randomly and the total field is calculated using Eq. (4), allowing the energy change ΔE to be calculated. After a number of such moves the system evolves into a thermal equilibrium configuration characteristic of the behavior of SPM particles, but in this case taking into account interactions via the local field, which of course introduces a coupling between the SPM and thermally stable components of the magnetization.

It is important to note that the SPM behavior persists up to large energy barriers (typically, for a measurement time of 100 s up to a value of $25kT$). Essentially this creates difficulties for the standard MC approach, since a moment is likely in practice to become localized in one or other of the energy minima resulting in apparent nonequilibrium behavior as an artifact of the unreasonably large number of Monte Carlo moves necessary to achieve equilibrium. Although in principle the SPM system would achieve thermal equilibrium, the computational time required is prohibitively long, due to the small transition probabilities involved. Essentially, for large energy barriers we can consider the particle as a two-state system, since the orientational distribution of the magnetic moments is clustered around the energy minima. SPM behavior is a result of the rapid transitions between the minima, which allow thermal equilibrium to be achieved. Consequently an improved approach to the computational treatment of SPM particles with relatively large energy barriers can be derived by consideration of the relaxation of the magnetic moment described in general terms by the master equation for a two-state system¹⁵

$$dn_1/dt = n_2/\tau_{21} - n_1/\tau_{12}, \quad (5)$$

where n_1 and n_2 are the numbers of particles in states 1 and 2, and τ_{12} and τ_{21} are the relaxation times between the two states. It is straightforward to show that the solution of Eq. (5) leads to a time dependent probability of the form

$$p_i(t) = \tau_{ij}^{-1}/\tau^{-1} + [p_i(0) - \tau_{ij}^{-1}/\tau^{-1}] \exp(-t/\tau), \quad (6)$$

where p_i is the probability of occupation of state i , and $\tau^{-1} = \tau_{12}^{-1} + \tau_{21}^{-1}$ is the total relaxation time for the system. The condition for thermal equilibrium (SPM) behavior in this case is $t/\tau \gg 1$, leading to the expression

$$p_i = \exp(-E_i/kT) / [\exp(-E_1/kT) + \exp(-E_2)], \quad (7)$$

where E_i is the energy of state i . Using the standard MC technique of importance sampling it is easily possible to generate the correct populations in each state. However, the master equation approach does not include the inevitable distribution of the magnetic moment about the local energy minimum. In our simulations, we carry out standard MC moves about the minimum in order to achieve a correct thermodynamic description of the magnetic microstate. It should

be noted that the master equation approach works well down to energy barriers $\approx 3kT$. For energy barriers approaching this value, the distribution of magnetic moments around the energy minimum becomes significant. Essentially, the inclusion of MC moves around the equilibrium position ensures a smooth transition into the separate computational approach used for $E_b \leq 3kT$.

The magnetization reversal for a blocked particle takes place by a transition over the energy barrier. This is modeled by calculating the transition probability given by

$$P_r = 1 - e^{-t_m/\tau}, \quad (8)$$

where t_m is the measuring time and τ is the relaxation time. In general τ^{-1} is given by the Arrhenius-Neel law [Eq. (1)], where $E_b(H_T, \bar{\psi})$, the height of the total energy barrier for reversal is a function of the particle orientation. Here $\bar{\psi}$ represents the orientation of the easy axis with respect to the total field. The angular dependence is specifically included because the model allows any arbitrary orientational distribution of easy axes and consequently E_b also depends on $\bar{\psi}$. The frequency factor $f_0 \approx 10^9 \text{ s}^{-1}$ is taken as a constant since this factor is slowly varying with field and the behavior of the relaxation time is dominated by the exponential function.

A simple analytical expression for the energy barrier when the easy axis is oriented at an angle with respect to the field is not obtainable. However in this case an approximate expression for $\Delta E(H_T, \bar{\psi})$ has been given¹⁶ as

$$E_b(H_T, \bar{\psi}) = KV[1 - h_T/g(\bar{\psi})]^{\kappa(\bar{\psi})}, \quad (9)$$

where $g(\bar{\psi}) = [\cos^{2/3}\bar{\psi} + \sin^{2/3}\bar{\psi}]^{-3/2}$ and $\kappa(\bar{\psi}) = 0.86 + 1.14g(\bar{\psi})$. Equation (9) was used to calculate transition probabilities via Eq. (8). A transition was allowed with a probability P_r by generating a random number x ($0 < x < 1$) and allowing reversal if $P_r > x$.

For particles which make the transition it is necessary to determine the new direction of the energy minimum. This was achieved by rotating our coordinate system so that the local field was along the z axis, thereby simplifying the location of energy minima.

In small fields such that the moment lies close to the easy axis the S-W equation has an approximate analytical solution which is¹⁷

$$\bar{\alpha}_{\min} = \sin^{-1} \left(\frac{h_T \sin \bar{\psi}}{1 + h_T \cos \bar{\psi}} \right), \quad (10)$$

where $\bar{\alpha}_{\min}$ is the angle between the applied field and magnetic moment in the rotated co-ordinates. Previous calculations¹⁸ have shown that Eq. (10) is approximately valid over a large field range. Where necessary the solution for $\bar{\alpha}_{\min}$ was refined numerically using the Newton-Raphson technique, requiring generally at most two iterations to achieve sufficient accuracy. After the determination of the energy minimum the direction was transformed back to the original coordinate system. As mentioned previously thermal activation leads to a Boltzmann energy distribution within

the energy minimum. Consequently, following the transformation back to the original coordinate system, standard Metropolis MC moves around the equilibrium position were carried out.

Thus, based on consideration of the relaxational behavior of individual particles a formalism is possible which encompasses both the reversible and irreversible phases of a fine particle system. In the following we apply the model to the study of reversible and irreversible behavior in strongly interacting fine particle systems. In order to achieve a detailed understanding of the behavior of the system, we also consider the temperature dependence of the initial susceptibility. This is finally interpreted in terms of the energy barrier distribution (and its dependence on the interactions) using the representation of the energy barrier distribution as the differential of the temperature decay of remanence curve.

III. RESULTS AND DISCUSSION

We have carried out an extensive study of the magnetic behavior of a system of interacting Co particles in order to gain a fundamental understanding of the effects of interactions on the reversible and irreversible magnetic behavior. The bulk of the investigation is dedicated to the temperature dependence of the magnetic properties, which have been the subject of considerable experimental study. The aim is to provide model calculations as a framework for understanding the experimental studies and also to elucidate the very subtle effects of interactions in granular magnetic solids. We start with a description of the room temperature properties. The system consisted of 1000 particles placed into a cubic computational cell as described earlier. The convergence of the calculations depends on a number of factors. Principally we are concerned with achieving the correct thermal equilibrium properties of the SPM fraction. As mentioned previously, this is somewhat complicated by the presence of large energy barrier of up to $25kT$ for the SPM particles. Our hybrid solution to this problem for particles with $KV/kT > 3$ consists of carrying out preliminary moves in which the particles are treated as a two-state system, with moves allowed only between the energy minimum positions. Because of the low number of degrees of freedom involved this was found to achieve equilibrium rapidly in a maximum of around 10–20 moves per particle. The system was then subjected to standard MC moves in order to allow thermal equilibrium to be achieved within the minima, which required typically 200–250 moves per particle. The correctness of this approach was established by carrying out calculations for a system of noninteracting SPM particles, for which the reduced magnetization (relative to saturation) is given by

$$\bar{M}(\mathbf{e}) = \frac{\int \int \sin \theta \exp(-E/kT) d\theta d\phi}{\int \int \exp(-E/kT) d\theta d\phi}, \quad (11)$$

where we note that the magnetization is a function of the orientation (\mathbf{e}) of the easy axes. E is given by Eq. (2), noting that, in the absence of interactions $\mathbf{H}_T = \mathbf{H}_a$ with the applied

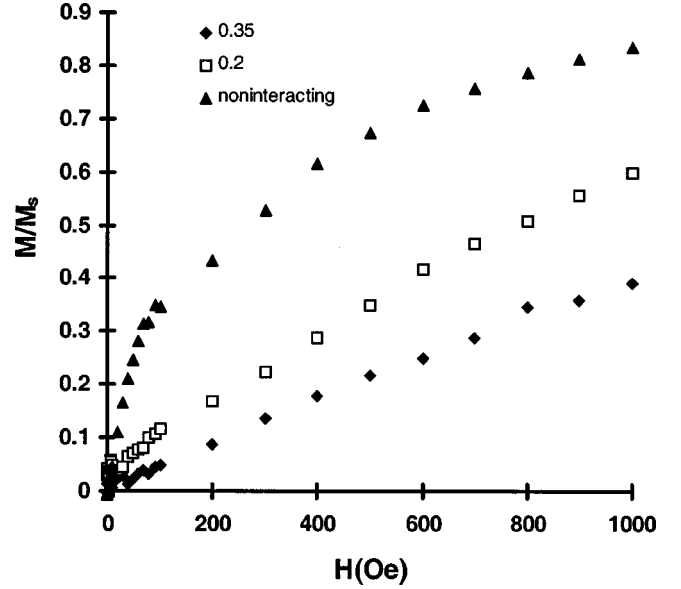


FIG. 1. Magnetization curves for a system of SPM Co particles with a median diameter of 7 nm and standard deviation of 0.15, at different packing densities

field oriented along the z axis. Equation (11) was evaluated numerically for comparison with MC calculations using the hybrid approach for a noninteracting system of particles, which was found to give good agreement. This procedure is clearly vital in validating and testing the numerical implementation of the hybrid approach.

Calculations of the variation of magnetization with field for a system of fine cobalt particles are shown in Fig. 1. The parameters used correspond to bulk cobalt ($M_s = 1400$ emu/cc and $K = 4 \times 10^6$ erg/cc) with a median diameter of 7 nm and standard deviation of the (lognormal) distribution of 0.15. This relatively large size corresponds to those observed in solidified ferrofluids and is chosen to illustrate a number of features, which are clear in Fig. 1. First it can be seen that there is a strong variation of magnetization with packing density. For the noninteracting case, the form of the variation of magnetization with field deviates significantly from the Langevin function normally expected for superparamagnetic materials. The reason for this is the effect of the material anisotropy on the magnetization curve.¹⁹ Although the initial susceptibility is independent of the material anisotropy, at larger fields the anisotropy tends to restrict the magnetic moments to the easy direction and to lower the magnetization in a given field. This gives rise to a change of slope in the magnetization curve at around a reduced magnetization of 0.35 as is evident in Fig. 1. The reduction in susceptibility at higher packing density is due to the effect of the interparticle magnetostatic interactions. The reduction is a result of the formation of flux closure configurations which minimize the magnetostatic energy and which are highly stable against the action of the external applied field. It is also interesting to note that the interacting systems do not exhibit the change in gradient associated with the effects of anisotropy in the noninteracting case. This shows that the interactions dominate the magnetic state at the higher pack-

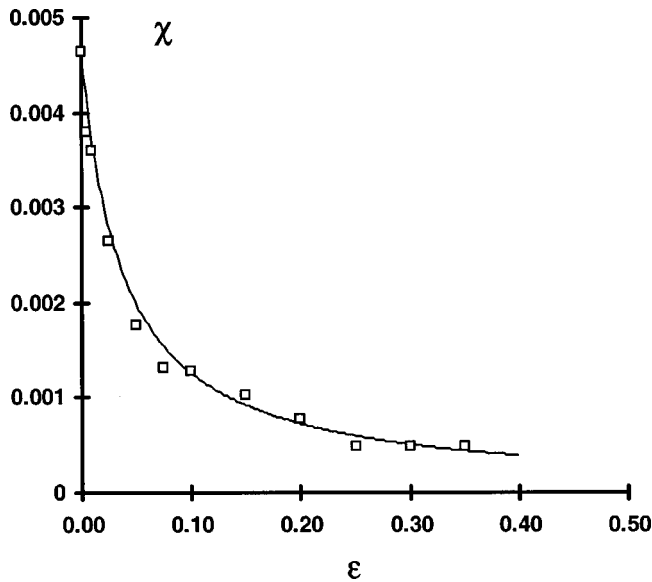


FIG. 2. The variation of susceptibility with packing density for 7 nm diameter Co particles.

ing densities; an observation which is important for the interpretation of the temperature dependence of the susceptibility.

We have also calculated the variation of initial susceptibility with packing density for the cobalt particle system and the results are shown in Fig. 2. It can be seen that there is a dramatic reduction in susceptibility as the packing density changes from the noninteracting case to a packing density of 0.35. It can be seen that the variation is highly nonlinear. As mentioned previously the reduction in susceptibility arises from the production of flux closure configurations in the demagnetized state, due to the magnetostatic interactions. It has been found important to correctly simulate the demagnetized state. Simply assigning directions at random to the magnetization leads to a high energy state which is relatively easily magnetized. This is a nonphysical situation, which we have avoided by carrying out an annealing of the configuration in order to produce a realistic demagnetized state.

In all numerical calculations system size can have an important effect. It is interesting to note here that the first manifestation of system size effects appeared, in this study, in the production of the demagnetized state. The initial (room temperature) calculations were possible for packing fractions as high as 0.35. However, at low temperatures, as will be discussed later it was found impossible to produce realistic demagnetized starting states for the ZFC magnetization calculations for the system size used here, presumably because of the increasing correlation lengths. For a system size of 1000 particles ZFC calculations were limited to packing densities $\epsilon < 0.2$. In order to extend the calculations significantly larger system sizes will be required.

We now proceed with a detailed investigation of the susceptibility of an interacting fine particle system, first by calculations of the variation of initial susceptibility χ with temperature. It is known that the initial susceptibility exhibits a characteristic peak as the particles change in terms of their magnetic behavior from being SPM at high temperatures to

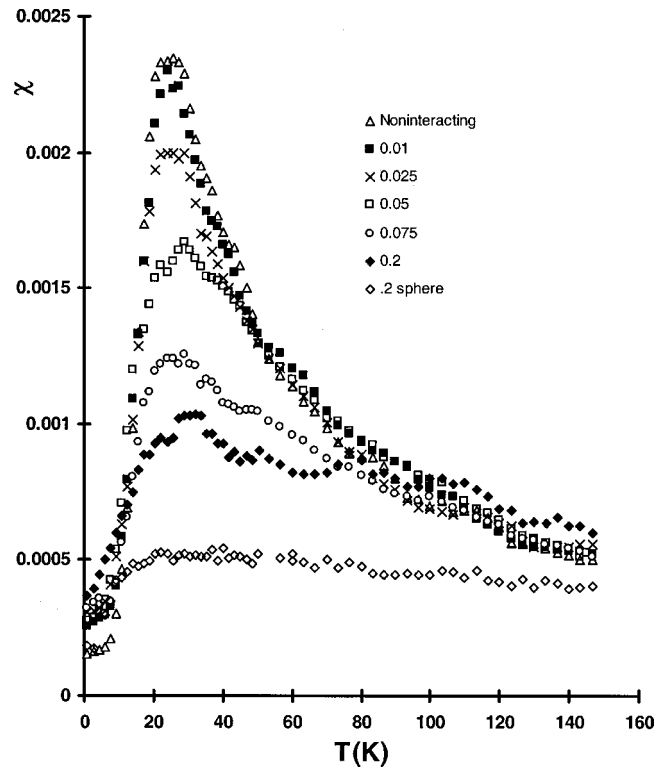


FIG. 3. Susceptibility vs temperature for various packing densities for Co particles with median diameter 3 nm and standard deviation 0.1. Values of packing density are indicated in the legend.

being ferromagnetically stable or “blocked” at lower temperatures. This has been observed in a number of materials.^{20,21} Although the analogy between spin-glass behavior and that of a fine particle system has often been made, it has also been pointed out²² that there are a number of differences between the properties of a fine particle system and that of a canonical spin glass. The following investigations have been carried out to assess the effect of short and long range interactions on the magnetic properties. The long range interactions are exemplified by studying the difference between thin-film samples and bulk samples in the form of a sphere for which a demagnetizing factor of $4\pi/3$ must be applied. The particles are assumed to have the bulk saturation magnetization and anisotropy constant of cobalt.

Figure 3 shows the susceptibility versus temperature for various packing densities up to 0.2. The calculated curves show the expected peak in the susceptibility at a temperature of around 23 K for the noninteracting system. The polydispersity of the samples is evident in the relatively broad peak. The effect of interactions is to give rise to a dramatic reduction in the susceptibility as the packing density increases. There is also a significant broadening of the curve with increasing ϵ . This is consistent with an increase in the width of the effective energy barrier distribution due to interaction effects, itself a result of a dispersion in the magnitude and direction of the local interaction field. This dispersion is clearly important in determining the magnetic properties of the system. There is evidence that the susceptibility at low temperatures increases with packing density, which can be broadly interpreted in terms of the wider energy barrier dis-

tribution. It also implies that a fraction of the particles in the low temperature microstructure have a relatively high susceptibility. This is consistent with the frustration arising from competing positive and negative interactions as will be discussed more fully later in relation to calculations of the spin-spin correlation function. The prediction of a broadening and flattening of the susceptibility/temperature curve is consistent with the results of Taketomi²³ on frozen ferrofluids, who found that systems with a tendency to cluster formation in fact exhibited no susceptibility peak. The tendency of our simulations is certainly toward this case, although at the packing densities achieved here we would not expect the interaction effects to be as strong as in a fully aggregated ferrofluid, and therefore we would not expect the simulations to exhibit such extreme behavior.

It should be noted at this point that the variation of χ with T depends very strongly on the low temperature initial state. Simply assigning initial moment directions at random at the lowest temperature gives, we believe, nonphysical results arising from the far from equilibrium initial state. Within the model calculations it was necessary to carry out a controlled cooling of the sample from temperatures in excess of 200 K down to the starting temperature of 1 K. For the strongly interacting systems the rate of reduction of the temperature and also the temperature step used was found to be crucial. All initial states were produced by very slow cooling. For $\varepsilon < 0.2$ it was possible to produce demagnetized configurations with reduced magnetization smaller than around 0.03. This was considered to be satisfactory from the point of view of calculating initial susceptibility vs temperature curves. Above this packing density it was found increasingly difficult to produce correctly demagnetized samples, due to increasing correlation lengths in the system. Thus, our current investigation is limited to $\varepsilon < 0.2$. Extending the range of the model to higher packing densities is in principle possible, but would require excessive computational times. The data presented in Fig. 3 is predominantly for a thin-film sample, with a demagnetizing factor of zero. The effect of long-range interactions is demonstrated by including the curve calculated for a spherical sample at a packing density $\varepsilon = 0.2$. The reduction in the susceptibility due to the demagnetizing field is clear.

There are two characteristic temperatures associated with the variation of χ with T which are often studied experimentally. The first of these is the temperature T_g at which the susceptibility peak occurs. This we find to be dependent on the packing density as shown in Fig. 4. The variation is rather nonlinear with a functional dependence $T_g \propto \varepsilon^{1/2}$. The solid line in Fig. 4 is the corresponding fit. The solid symbols in Fig. 4 correspond to simulations carried out with a spherical sample, and the open circles are calculations for a film. Within the statistical errors of the calculation there is no significant difference between the sphere and the film indicating that in this case the long range interaction effects are having a relatively small effect on T_g : the most significant effect of the demagnetizing interactions is an overall depression of the susceptibility. Clearly for cobalt systems the susceptibility is strongly affected by nearest-neighbor interactions. Previous work^{6,22} has demonstrated experimentally an

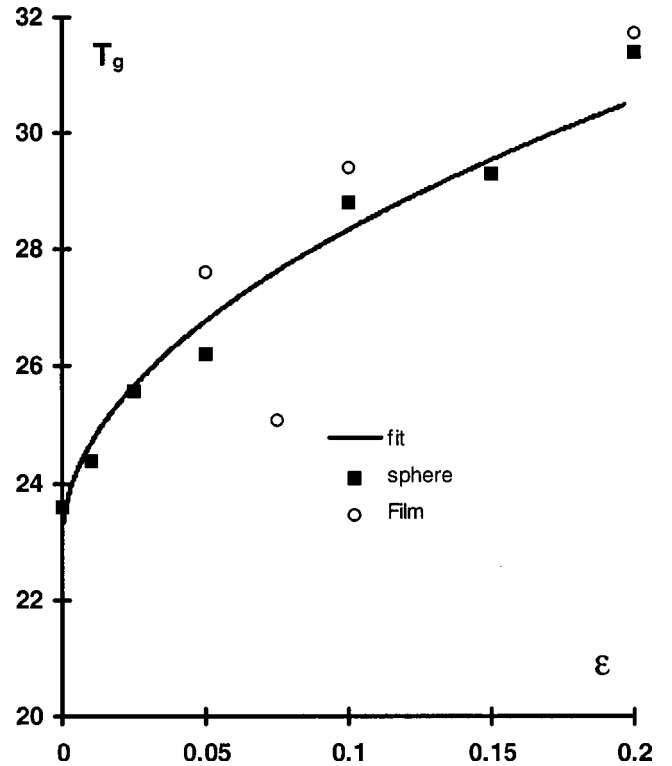


FIG. 4. The dependence of T_g on the packing density ε . There is at most a weak dependence of T_g on the long range interactions. The solid line is a fit to $T_g \propto \varepsilon^{1/2}$.

increase in the T_g with packing density. In the case of Ref. 6 the power law experimentally had an exponent closer to 0.17. However, these experiments were for well dispersed Fe_3O_4 particles, which might be expected to be less strongly interacting than Co because of their lower saturation magnetization.

The effects of magnetostatic interactions are also investigated by means of an ordering temperature T_0 calculated from the high temperature SPM regime. In the absence of interactions it is expected that in this region the SPM system would obey the Curie-like law $\chi = C/T$. Figure 5 shows plots of χ^{-1} vs T for a spherical sample with various packing densities. The plots are reasonably linear for $T > 50$ K. It is clear from Fig. 5 that magnetostatic interactions give rise to an apparent ordering temperature T_0 which is negative and whose magnitude increases with packing density. The variation of T_0 with packing density is shown in Fig. 6, which demonstrates for this particular characteristic temperature a much stronger dependence on the long-range interactions. The large negative values of ordering temperature might be interpreted as indicating some ‘‘antiferromagnetic’’ order. While we believe this is a possibility in systems with a relatively well ordered lattice which could exhibit the required order in the form of interpenetrating sublattices we believe that this is not the case in our disordered system. Correlation functions indicate a relatively short-ranged order consisting of flux closure configurations with low magnetostatic energy. In strongly interacting systems the magnetostatic energy is sufficient to dominate over the anisotropy energy, as indicated by the room temperature calculations given in Fig. 1,

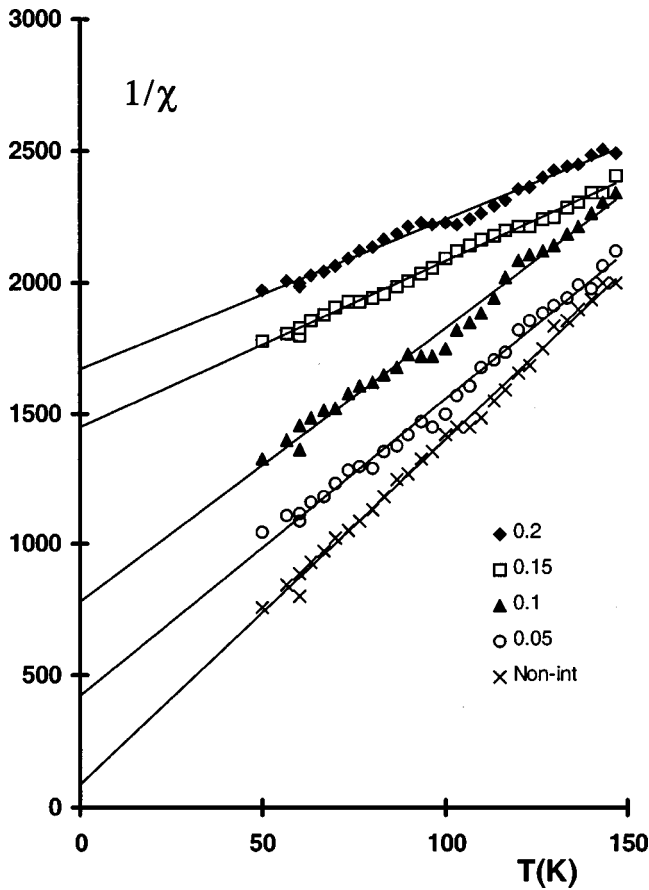


FIG. 5. Plots of χ^{-1} as a function of T for different packing densities as indicated in the legend. All plots are in the linear region, i.e., from for $T > 50$ K which is $\approx 2T_g$.

leading to a relatively broad χ vs T curve. Direct evidence of short-ranged order using a spin-spin correlation function will be given later.

We now consider the effect of an applied magnetic field on the dc susceptibility. The applied dc field has the effect of

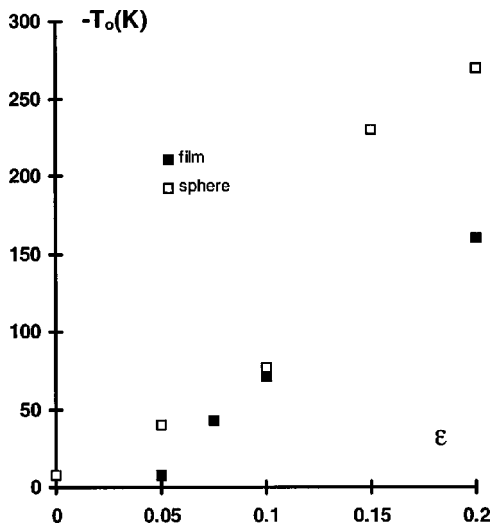


FIG. 6. The variation of the negative ordering temperature T_0 with ϵ . The solid symbols are for the thin film calculations. T_0 is strongly dependent on the long range interactions.

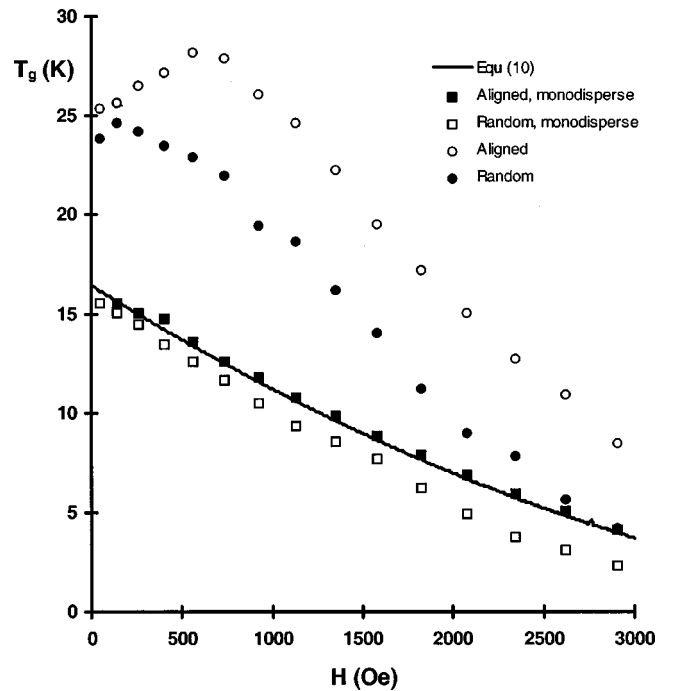


FIG. 7. Calculations of T_g as a function of H for a noninteracting system of Co particles with 3 nm median diameter, both monodispersed and with $\sigma=0.1$, for randomly oriented and aligned systems. T_g is strongly dependent on the orientational texture of the material and also on the presence of a dispersion of particle size.

lowering the anisotropy energy barrier, which leads to a lower temperature at which the peak in the dc susceptibility occurs. This is a well known result, which has been extensively studied experimentally. Generally speaking, theoretical studies have been based on a system of aligned particles for which semianalytical approaches are possible. For example, Wenger and Mydosh²⁴ have used the relaxation time expression given by Brown²⁵ to carry out numerical calculations which show a power law dependence of the blocking temperature of the system on the field, of the form $T_b \propto H^\delta$ where $\delta=2$ for low fields and $\delta=2/3$ for high fields. For the frozen state of a spin-glass similar expressions have been predicted by Toulouse and Gabay²⁶ and Almeida and Thouless.²⁷ Previous experimental work given in Ref. 7 has given reasonably good agreement with these expressions but also indicates that interactions have a strong bearing on the experimental results. Here, we first consider the case of a noninteracting system since our numerical results allow an exploration of the effects of particle orientation on the field dependence of the dc susceptibility. The results are summarized in Fig. 7 which gives calculated results for aligned and random systems, both monodispersed and with a lognormal particle size distribution having a standard deviation of 0.1. The peak temperatures for the system with a particle size distribution are generally higher as has been noted previously.⁷ The solid line in Fig. 7 has been calculated using the following expression for the field dependence of the blocking temperature:

$$T_B(H) = T_B(0)(1 - H/H_K)^2. \quad (12)$$

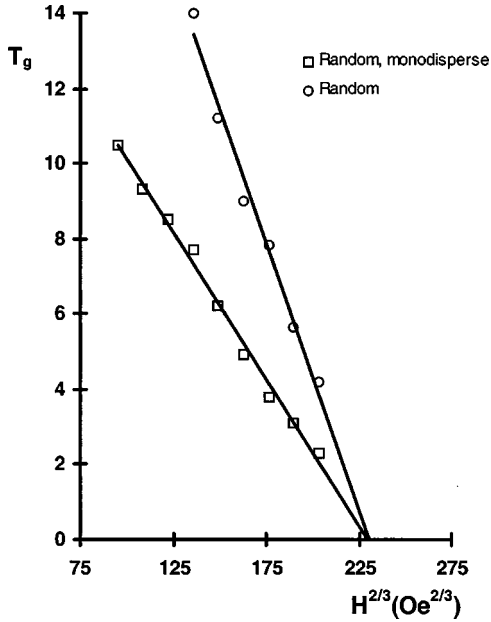


FIG. 8. The variation of T_g with $H^{2/3}$ in large fields for the noninteracting system of Fig. 7, the solid lines being a least squares fit to the calculated results.

As expected, Eq. (12) gives good agreement with the numerically calculated data for the aligned and monodispersed system. For the monodispersed system we expect that the blocking temperature T_B should be equal to the peak temperature T_g . It is interesting to note that in the case of an aligned polydispersed system there is an initial increase in T_g leading to a maximum value at around 750 Oe. In order to explain the origin of this peak consider the following expression for the low field magnetization of the system

$$\bar{M} = \int_0^{y_p(H)} F(b)f(y)dy, \quad (13)$$

which represents an integration over the superparamagnetic part of the system with a distribution function written as $f(y)$ where $y = D/D_m$ and V_m is the corresponding medium volume. $f(y)$ is a volume fraction distribution, with $f(y)dy$ giving the fraction of the total magnetic volume having diameters between y and $y + dy$. \bar{M} is the reduced magnetization relative to the saturation magnetization of the sample. The function F of argument $b = I_{sb}VH/kT$ is the Langevin function for a randomly oriented system or $F = \tanh b$ for a system with aligned easy axes. Determination of the peak temperature as a function of H numerically from Eq. (13) demonstrates the existence of a maximum. The maximum is evident for the aligned system with a weaker peak for the randomly oriented case. The existence of the peak is sensitive to the width of the particle size distribution, disappearing rapidly as σ increases. Further insight into the predicted peak can be obtained from the linearised form of Eq. (13) appropriate for small fields. The condition for the temperature maximum at a given value of field H follows as

$$\int_0^{y_p(H)} y^3 f(y) dy = \frac{1}{3} [y_p(H)]^4 f[y_p(H)]. \quad (14)$$

Numerical solution of Eq. 14 gives no peak as a function of the applied field. This suggests that the peak is a result of the nonlinear terms in the magnetization, as also shown by Hanson *et al.*²⁸ The polydispersed system with randomly oriented easy axes shows no strong evidence of a peak in the field variation of T_g . This is presumably a result of the spread of energy barriers introduced by the random orientation of the easy axes. We note that the work of Luo *et al.*²² does show evidence of a peak in agreement with this prediction. This may indicate some preferential alignment of the easy axes in their experimental systems, since the peak is not present in a randomly oriented system.

Figure 8 gives plots of T_g vs $H^{2/3}$ for the monodispersed and polydispersed systems with randomly oriented easy axes. Interestingly these systems obey an $H^{2/3}$ law, which indicates that the experimentally observed $H^{2/3}$ law is attributable at least in part to the random orientation of the easy axes. Both the polydispersed and monodispersed systems extrapolate to the same effective value of H_k of 3.5 kOe, which is slightly higher than half the calculated value of H_k for the system.

Essentially, the field variation of T_g is dependent predominantly on the field dependence of the average energy barrier of the system. This is the premise behind all previous

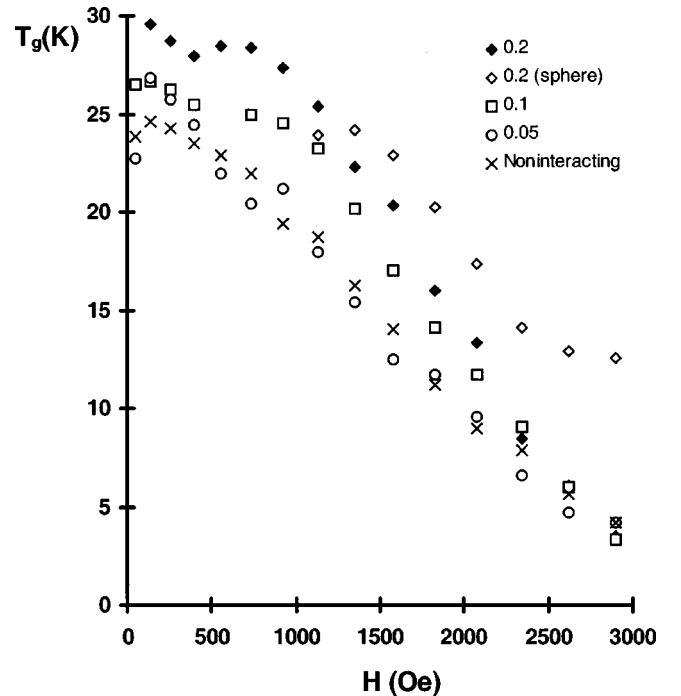


FIG. 9. The variation of T_g with H for systems of different packing densities as indicated in the legend. The effect of interactions is to increase the curvature of these plots which is indicative of the effect of interactions on the variation of energy barrier with H . The long-range interactions as represented by the calculations for a sphere at $\varepsilon = 0.2$ show a large deviation from the calculations from a thin film at large values of H .

attempts to calculate analytically the variation $T_g(H)$. The results of our calculations are summarized in Fig. 9, which gives the variation of $T_g(H)$ for various packing densities. Overall, the results are consistent with the experimental data of Luo *et al.*²² Specifically, interactions dominate the properties for small applied fields, with the curves merging at large H . This is not unreasonable as one would expect the applied field to dominate over the nearest neighbor interactions as the system approaches saturation. For comparison, we include calculations for a spherical sample (only the high field data are shown for clarity)—in small fields the two sets of results merge as expected). For the spherical sample the demagnetizing field has a large effect on the behavior of the system at large fields. This effect of course can be included by a mean-field approach. Of more importance is the dependence on packing density at low fields. This implies that interactions are having a strong bearing on the effective energy barrier dispersion of the material especially at small fields. There is some evidence in the noninteracting case of a small peak in low fields, as was observed and noted by Luo *et al.* The effect of interactions is to remove this peak at the higher packing densities. There is some evidence for a reduction of the peak in the data of Luo *et al.* although we note that their experimental data were for relatively weakly interacting magnetite particles at low density.

It should be stressed that the effect of interactions in the calculations described so far is invariably to increase the effective energy barrier of the system. Specifically, an increase of the peak temperature with packing density is observed and there is an increase in curvature of the T_g vs H plot as the packing density increases, indicating a strong effect of the interactions on the form of the variation of energy barrier with field. It is interesting to note that in the case of the strongly interacting systems the variation in small fields is rather slow. This compares markedly with the noninteracting case and is in fact more similar to the weak dependence of T_g on H for small fields in the canonical spin-glasses AgMn and CuMn.²⁹

We also find strong effects of interactions in a comparison between the field cooled magnetization (FC) and the zero field (ZFC) magnetization. The ZFC magnetization essentially represents the dc susceptibility and is obtained by the application of a static magnetic field at a low temperature after which the sample is progressively warmed beyond the maximum in the susceptibility T_g . The FC magnetization was obtained by applying a field and cooling the sample from a temperature well above T_g (in this case 150 K) down to a temperature $T=1$ K. Thus the FC magnetization is achieved by a dynamic process, in which the relaxation behavior of the particles might be expected to play a significant role. Consequently, the FC magnetization should depend upon the rate at which the temperature is reduced. Experimentally such behavior has been observed by Wenger and Mydosh³⁰ in an insulating spin glass system. A theory giving an expression for the FC magnetization of a fine particle system was given by Chantrell and Wohlfarth.³¹ The result is a rate dependent critical temperature at which the system makes a transition from being superparamagnetic to being ferromagnetically stable. The situation regarding the effects

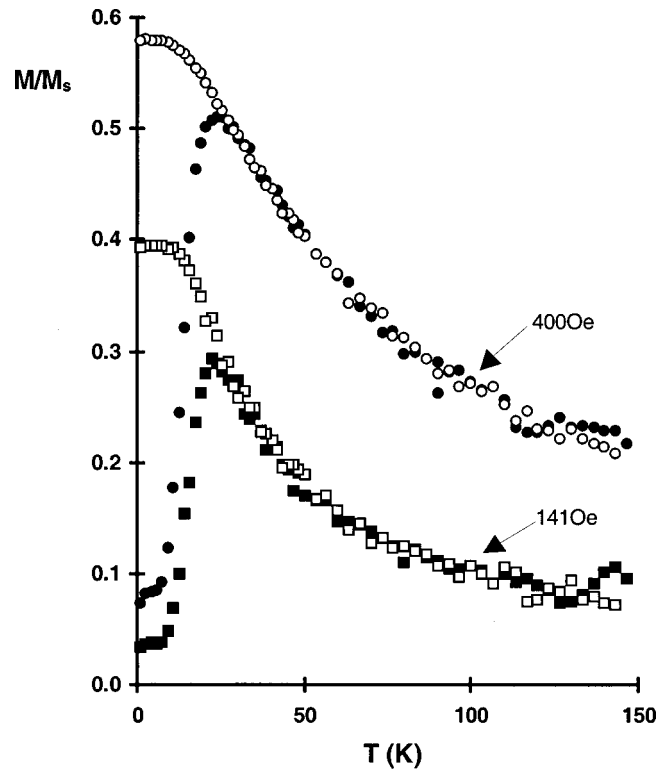


FIG. 10. A comparison of the FC and ZFC magnetization for a noninteracting system at fields of 141 and 400 Oe. Open symbols represent FC, and closed symbols ZFC magnetization, respectively.

of interactions in such a system is very poorly understood. Recently, Dormann *et al.*⁴ have reviewed some experimental data relating to γ -Fe₂O₃ particles in a polymer. Their conclusion is that for weakly interacting systems there is a relatively strong increase in the FC magnetization at low temperatures which tends to be reduced by the effects of interactions. Interestingly a weak maximum in the FC magnetization in some samples was also noted by these authors. Dormann *et al.* also note that no model of the FC magnetization has been produced taking into account specifically the interparticle interactions, which makes the interpretation of experimental data extremely difficult.

Our model allows the calculation of the ZFC and FC magnetization. Figure 10 shows calculations for two applied fields of the ZFC magnetization and FC magnetization for a noninteracting system. As expected, above T_g the two curves merge. The divergence occurs at a temperature slightly greater than T_g , which is a reflection of the volume distribution of the system. The size distribution assumed in our model is relatively narrow. We would expect that as the size distribution increases in width the two curves would diverge at temperatures significantly larger than T_g . The FC magnetization decreases to a plateau at a temperature somewhat less than T_g . These observations are consistent with the theoretical approach given in.³¹ It is interesting to note that the data represented in Refs. 4 and 22 show a continuous increase of the FC magnetization with decreasing temperature. This may reflect relatively large particle size distributions in these systems. The effect of interparticle magnetic interactions is quite dramatic as shown in Fig. 11. Here we show

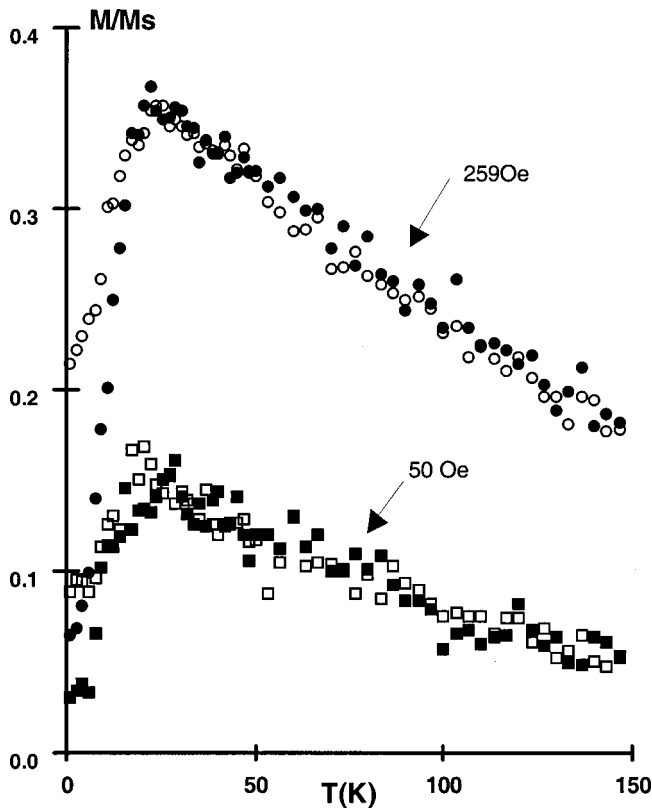


FIG. 11. A comparison of the ZFC (solid symbols) and FC (open symbols) magnetization for an interacting system with $\varepsilon = 0.1$ and two applied fields. The presence of a peak in the FC magnetization is clear.

calculated results for the interacting system of cobalt particles in fields of 50 and 259 Oe, both ZFC and FC magnetization. Data in Fig. 11 are for a packing density of 0.1. It can be seen that the interactions give rise to a peak in the FC magnetization. This is consistent with the observation of Ref. 4 and also with data presented by Greaves *et al.*³² on AgNiFe alloy films. We assume that these are relatively strongly interacting systems because of the Fe content, which would explain the relatively strong peaks observed in the systems. It can be seen from Fig. 11 that the ZFC and FC magnetizations diverge at a relatively low temperature for the 50 Oe field. At the larger field the two curves become more separated. The results for a packing density of 0.2 are given in Fig. 12, which demonstrate a similar effect. In addition, as the field increases the peak in the FC magnetization becomes less pronounced. This is consistent with interactions having a smaller effect on the functional form of the energy barrier at larger fields analogous to the previous observations of the variation of T_g with H .

We note that so far all the results obtained can be interpreted in terms of an increase in the width of the energy barrier distribution due to interactions and a shift of the average energy barrier to higher energies. However, we conclude this investigation by studying the energy barrier distribution by the use of the remanent magnetization. Here, we look at two types of remanent magnetization. The first is the remanence obtained by cycling the sample through a hysteresis

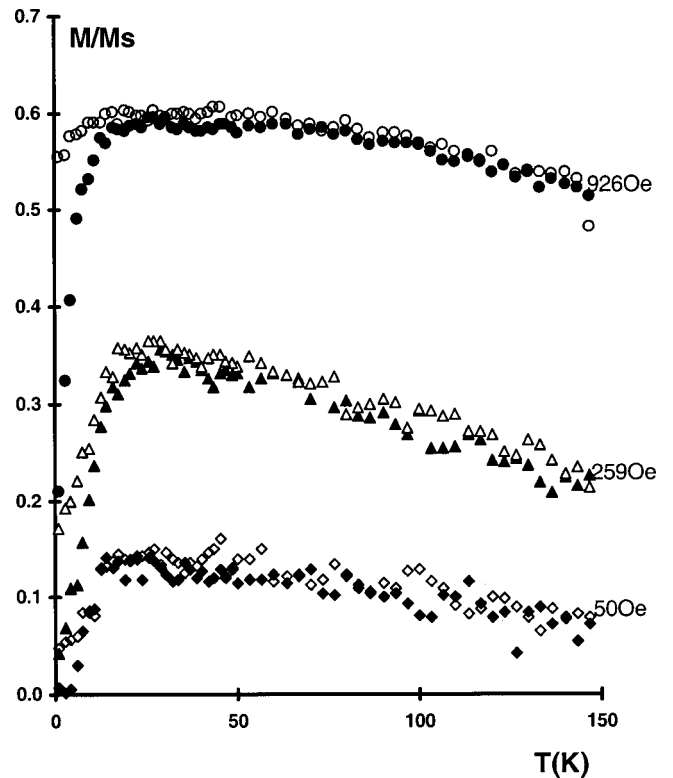


FIG. 12. ZFC magnetization (solid symbols) and FC magnetization (open symbols) for different fields at a packing density of $\varepsilon = 0.2$. At small fields the interactions completely dominate the system. At larger fields the peak in the FC magnetization becomes rather less pronounced.

loop to the remanent state at very low temperature, followed by a gradual increase of the temperature and a measurement of the magnetization. This is the commonly used temperature decay of remanence curves, which can be related to the energy barrier distribution. The second is referred to by Blythe *et al.*³³ as hysteresis loop remanences (HLR). In this case the sample is cycled through the hysteresis loop to remanence at each temperature concerned. Blythe *et al.* noted a difference between the two types of remanent magnetization. Our results are shown in Fig. 13. The magnetostatic interactions introduce a dramatic reduction of the remanent magnetization. The remanence in this case is reduced by a factor of 2 for a system with a packing density of 0.01. Two further factors are interesting to note. The noninteracting case exhibits a large plateau at low temperatures. This is a result of the narrow particle size distribution in our system. However, as the packing density increases this plateau essentially disappears and the system simply exhibits a rapid decrease of the remanent magnetization with increasing temperature. This is consistent with most experimental data, where a plateau is in general not observed. It is clear from our computational results that the slope of the M_r vs T curve is strongly dependent on magnetostatic interactions even at very low densities. Consequently, energy barrier distributions determined by differentiation of such curves must be considered to be strongly influenced by the interparticle magnetostatic interactions. The effect of interactions can be

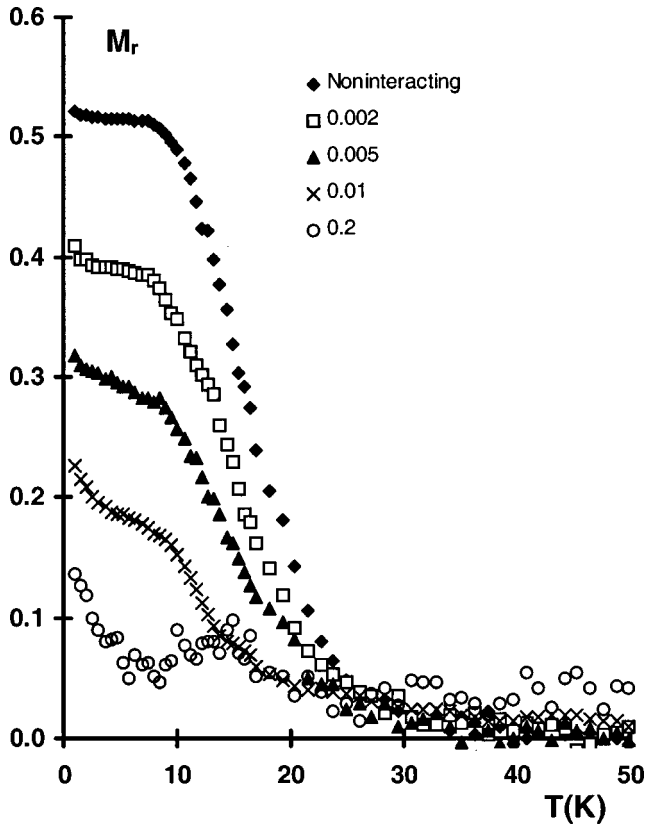


FIG. 13. Temperature decay of remanence curves for the Co fine particle system with various values of packing density ε as indicated in the legend.

characterized by the differential of the remanence curve with respect to temperature, which is a measure of the energy barrier distribution. In this case the distribution is found to shift to lower energy barriers. This is inconsistent with the inference of energy barriers increasing with interactions, which is the simple interpretation of the effect of interactions on the susceptibility/temperature curves of Fig. 2. This apparent inconsistency is in fact easily reconciled by the existence of shorted-ranged order, as will be discussed shortly. A final, very subtle effect of the interactions is demonstrated in Fig. 14 which compares the difference between the standard temperature decay of remanence and the HLR measurements carried out by Blythe *et al.* It can be seen that there is a significant difference between the two types of measurement which indicate strongly that the magnetic behavior is dependent on the state of the system. This is not a long range interaction effect since these calculations were made for a film geometry. Clearly, the remanent state at a given temperature produced by cycling the field into the remanent state is rather more stable than that obtained by the temperature decay of remanence. A difference between the two types of measurements was noted by Blythe *et al.* However, their data showed that in temperature decay of remanence measurements M_r extends to a very high temperature tail, which has not been observed in our simulations. Instead, we observe a small difference in the low temperature remanent magnetization values. A more detailed calculation working with the specific materials parameters of the work of Blythe

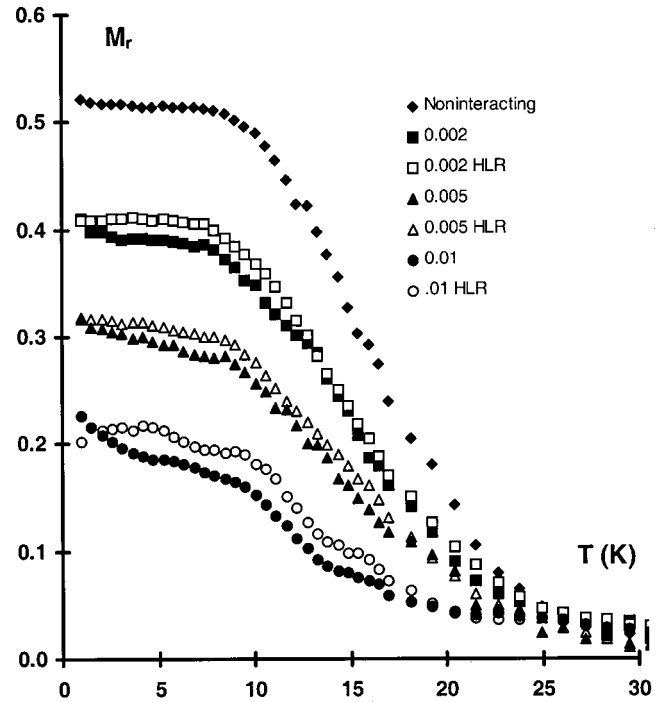


FIG. 14. A comparison of the temperature decay of remanence process with the HLR process. Values of packing density are indicated in the legend.

et al. is necessary in order to study the origin of this discrepancy. However, it is significant that both theory and experiment predict a difference between the temperature decay of remanence and the HLR, which is worthy of further study.

The computational results presented in this paper cannot be interpreted by a simple effective change in the energy barrier resulting from interactions. They can, however, be explained in terms of effective energy changes coupled with a slow transition to an ordered state at low temperatures. In our model system we can of course investigate this by means of correlation functions. Here we choose a correlation function defined as

$$\xi(r, \theta) = \langle \mu_i \cdot \mu_j \rangle,$$

with $\langle \rangle$ representing an ensemble average. The polar coordinates (r, θ) represent the position of particle j in a coordinate system based on the orientation of the moment of particle i . This definition makes ξ sensitive to local anisotropies in the magnetic microstructure such as small clusters, which would otherwise be lost.

Investigations show a gradual transition to a state with short-ranged (glassy) order at low temperature, with no evidence of a divergence in the correlation length. For clarity in Fig. 15(a) we show results for temperatures $T=300$ K and $T=1$ K (the starting point for the ZFC magnetization calculations), in zero applied field. The technique of batch means was used to calculate the mean value of and standard error in $\xi(r, \theta)$. Figure 15(a) shows $\xi(r)$ for $\theta=0$ and $\pi/2$, i.e., parallel and perpendicular to the local magnetization direction. $\xi(r)$ shows short-ranged order having positive values char-

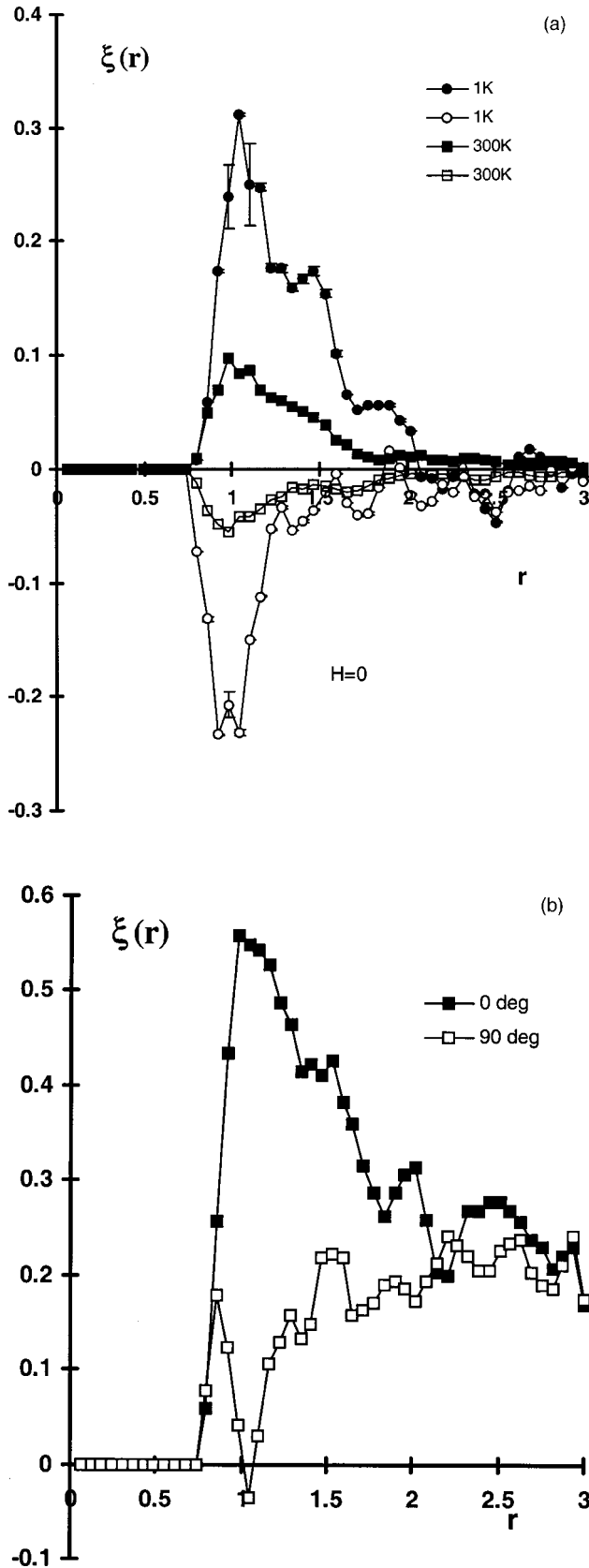


FIG. 15. Correlation functions parallel and perpendicular to the local magnetization (a) in zero field for $T=300$ and 1 K, and (b) for $H=921$ Oe at $T=1$ K. Closed symbols: $\theta=0$, open symbols: $\theta=\pi/2$.

acteristic of “ferromagnetlike” order for $\theta=0$ and negative values indicating antiferromagnetlike order for $\theta=\pi/2$. We stress that this order is rather local (demonstrated by the small correlation length) and also macroscopically isotropic. The anisotropy apparent in Fig. 15(a) is a local phenomenon, highlighted by our use of a “local” correlation function. Figure 15(a) is characteristic of short chains oriented locally antiparallel (but with randomly oriented chain axes) or of small flux closure loops. Either configuration is consistent with the low energy demagnetized state inferred from the susceptibility and remanence calculations. We note also that the correlation function demonstrates the presence of competing positive and negative correlations, leading to the presence of frustration, consistent with the increased susceptibility at low temperatures noted earlier.

Figure 15(b) gives results for a system with $\varepsilon=0.2$ cooled in a field of 921 Oe, corresponding to one of the FC magnetization curves in Fig. 12. It can be seen that the field cooled state has a rather different form of correlation function. For $\theta=0$ $\xi(r)$ is always positive, tending asymptotically to a finite value for large r . The same asymptote (related to the system magnetization), is reached for $\theta=\pi/2$. Clearly the applied field has reduced the negative correlations at $\theta=\pi/2$ by mitigating against the formation of local configurations of low magnetostatic energy. This is perfectly consistent with the reduction in the peak in the FC magnetization with increasing field. Clearly it cannot be expected that analytical treatment, neglecting the presence of correlations, will be successful in describing the properties of strongly interacting systems. Our results also demonstrate that the form of the correlations themselves vary in a complex manner with the external field and indeed the temperature history of the sample, which must be considered in the interpretation of experimental data.

IV. CONCLUSIONS

We have carried out an extensive investigation of the quasistatic magnetic properties of an interacting fine particle system, using a Monte Carlo model taking account of the complex combination of reversible and irreversible magnetic properties, which characterize its behavior. The model correctly predicts the form of the susceptibility/temperature curve and an increase of peak temperature T_g with ε , in agreement with experiment. A second characteristic ordering temperature T_o is found to be negative, increasing in magnitude with increasing ε . T_o is also found to be strongly dependent on the long-range interaction via the demagnetizing field term, in agreement with Ref. 4. We also find the presence of a peak in the FC magnetization. This arises from the tendency toward an ordered state at low temperatures having short ranged order characteristic of a spin-glass as described in Refs. 22 and 34. The broadening of the χ/T relationship and the shift of T_g to higher temperatures with increasing ε can be interpreted in terms of a modification of the effective energy barrier of the particle by the dipolar interaction. To some extent this is in agreement with analytical models proposed by Dormann and co-workers (reviewed in Ref. 4),

which essentially predicts increased energy barriers due to interaction. However, the behavior is extremely complex and subtle. For example, there is a significant increase in susceptibility with increasing ϵ at temperatures well below T_g . This could be associated with a form of frustration of the ordered magnetic configuration. Complete 3D flux closure, especially in a disordered system such as is studied here is extremely unlikely. It seems likely that the minimum energy state will involve positions of relatively high energy. A 2D analog of this is the central particle of a vortex structure produced by dipolar interactions, which is often observed to be weakly coupled to the vortex structure. Particles in high energy positions would be expected to exhibit an enhanced susceptibility consistent with our numerical results. A simple interpretation in terms of effective energy barriers is also excluded by the observation of a dramatically reduced remanent magnetization. This is more consistent with the transition to a magnetically ordered state involving a high degree of flux closure. The importance of a transition to an ordered state has been proposed by Hansen and Morup³⁵ and the numerical results presented here certainly underline this conjecture. It is clear that an understanding of the underlying magnetic state of the system is an important component of models of strongly interacting systems. Consequently the transition to the glassy state is worthy of extensive study. The importance of the magnetic state is also demonstrated by the predicted difference between the temperature decay of remanence and the HLR curves. It is also important to note that the transition to an ordered state carries the implication that for any property calculated starting at low temperatures

the correct simulation of the ground state is vital. We have found a strong dependence of the ZFC magnetization on the ground state. All calculations presented here were carried out using low temperature states produced by a slow cooling through the transition. The size of correlated regions essentially determines the upper limit of the packing density given the limitations of our system size. Essentially with 1000 particles a reasonable demagnetized state could not be produced for $\epsilon > 0.2$. At low temperatures there is a slow temporal evolution of the magnetic state, characterized by slow energy changes. This is presumably related to the aging effect observed in spin glasses and in fine particle systems.¹⁰

The dipolar interaction also has a strong bearing on the field dependence of the magnetic properties. As mentioned previously, the most dramatic effects of the transition to an ordered state are the existence of a peak in the FC magnetization and the rapid decrease of the remanence of the system. However, in addition, the nature of the ordered state gives rise to a large spread in the effective energy barrier distribution as reflected in a change in curvature of the T_g vs H relationship as the packing density increases.

ACKNOWLEDGMENTS

This work was carried out as part of the Technology Group 04 of the MOD Corporate Research Program. © British Crown Copyright 1999. Published with the permission of the Defense Evaluation and research Agency on behalf of the Controller of HMSO. The financial support of the UK EPSRC is gratefully acknowledged.

-
- ¹R. W. Chantrell and E. P. Wohlfarth, *J. Magn. Magn. Mater.* **40**, 1 (1983).
- ²J. L. Dormann, L. Bessais, and D. Fiorani, *J. Phys.: Condens. Matter* **21**, 2015 (1988).
- ³S. Shtrikman and E. P. Wohlfarth, *Phys. Lett. A* **85**, 467 (1981).
- ⁴J. L. Dormann, D. Fiorani, and E. Tronc, *Adv. Chem. Phys.* **XC-VIII**, 283 (1997).
- ⁵S. Morup and E. Tronc, *Phys. Rev. Lett.* **72**, 3278 (1994).
- ⁶M. El-Hilo, K. O'Grady, and R. W. Chantrell, *J. Magn. Magn. Mater.* **114**, 295 (1992).
- ⁷M. El Hilo, K. O'Grady, and R. W. Chantrell, *J. Magn. Magn. Mater.* **114**, 307 (1992).
- ⁸R. W. Chantrell, G. N. Coverdale, M. El-Hilo, and K. O'Grady, *J. Magn. Magn. Mater.* **157**, 250 (1996).
- ⁹J.-O. Andersson, C. Djurberg, T. Jonsson, P. Svedlindh, and P. Nordblad, *Phys. Rev. B* **56**, 13 983 (1997).
- ¹⁰T. Jonsson, J. Mattson, C. Djurberg, F. A. Khan, P. Nordblad, and P. Svedlindh, *Phys. Rev. Lett.* **75**, 4138 (1995).
- ¹¹D. Kechrakos and K. N. Trohidou, *Phys. Rev. B* **58**, 12 169 (1998).
- ¹²R. W. Chantrell, M. El-Hilo, and K. O'Grady, *IEEE Trans. Magn.* **MAG-27**, 3570 (1991).
- ¹³I. Neel, *Ann. Geophys. (C.N.R.S.)* **5**, 99 (1949).
- ¹⁴N. Metropolis, A. W. Rosenbluth, M. N. Rosenbluth, A. H. Teller, and E. Teller, *J. Chem. Phys.* **21**, 1087 (1953).
- ¹⁵I. Klik, C.-R. Chang, and J. Lee, *J. Appl. Phys.* **75**, 5487 (1994).
- ¹⁶H. Pfeiffer, *Phys. Status Solidi A* **118**, 295 (1990).
- ¹⁷K. O'Grady, R. W. Chantrell, J. Popplewell, and S. W. Charles, *IEEE Trans. Magn.* **MAG-16**, 1077 (1980).
- ¹⁸M. El-Hilo, R. W. Chantrell, and K. O'Grady, *J. Appl. Phys.* **84**, 5114 (1998).
- ¹⁹H. D. Williams, K. O'Grady, M. El-Hilo, and R. W. Chantrell, *J. Magn. Magn. Mater.* **122**, 129 (1993).
- ²⁰J. I. Gittleman, B. Abeles, and S. Bozowski, *Phys. Rev. B* **9**, 3891 (1974).
- ²¹C. L. Chen, *J. Appl. Phys.* **69**, 5267 (1991).
- ²²W. Luo, S. R. Nagel, T. F. Rosenbaum, and R. E. Rosensweig, *Phys. Rev. Lett.* **67**, 2721 (1991).
- ²³S. Taketomi, *Phys. Rev. E* **57**, 3073 (1998).
- ²⁴L. E. Wenger and J. A. Mydosh, *Phys. Rev. B* **29**, 4156 (1984).
- ²⁵W. F. Brown, Jr., *Phys. Rev.* **130**, 1677 (1963).
- ²⁶G. Toulouse and M. Gabay, *J. Phys. (France) Lett.* **42**, L103 (1981).
- ²⁷R. L. de Almeida and D. J. Thouless, *J. Phys. A* **11**, 983 (1978).
- ²⁸M. Hanson, C. Johansson, and S. Morup, *J. Phys.: Condens. Matter* **7**, 9263 (1995).
- ²⁹G. G. Kenning, D. Chu, and R. Orbach, *Phys. Rev. Lett.* **66**, 2923 (1991).
- ³⁰I. E. Wenger and J. A. Mydosh, *J. Appl. Phys.* **55**, 1717 (1984).
- ³¹R. W. Chantrell and E. P. Wohlfarth, *Phys. Status Solidi A* **91**, 619 (1985).

³²S. J. Greaves, M. El-Hilo, K. O'Grady, and M. Watson, *J. Appl. Phys.* **76**, 6802 (1994).

³³H. J. Blythe, G. A. Jones, and V. M. Fedosyuk, *J. Mater. Sci.* **31**, 6431 (1996).

³⁴S. Morup, F. Bodker, P. V. Hendriksen, and S. Linderoth, *Phys. Rev. B* **52**, 287 (1995).

³⁵M. F. Hansen and S. Morup, *J. Magn. Magn. Mater.* **184**, 262 (1998).